

Article

Heterotrophic Microbial Stimulation through Biosolids Addition for Enhanced Acid Mine Drainage Control

Omy T. Ogbughalu ¹, Andrea R. Gerson ², Gujie Qian ^{1,3}, Roger St. C. Smart ^{1,2}, Russell C. Schumann ^{1,4}, Nobuyuki Kawashima ³, Rong Fan ¹, Jun Li ¹ and Michael D. Short ^{1,3,*}

¹ School of Natural and Built Environments, University of South Australia, Mawson Lakes, SA 5095, Australia; omerebere.ogbughalu@mymail.unisa.edu.au (O.T.O.); Gujie.Qian@unisa.edu.au (G.Q.); Roger.Smart@unisa.edu.au (R.S.C.S.); Russell.Schumann@unisa.edu.au (R.C.S.); Rong.Fan@unisa.edu.au (R.F.); jun.li@unisa.edu.au (J.L.)

² Blue Minerals Consultancy, Middleton, SA 5213, Australia; Andrea.Gerson@bigpond.com

³ Future Industries Institute, University of South Australia, Mawson Lakes, SA 5095, Australia; Nobuyuki.Kawashima@unisa.edu.au

⁴ Levay and Co. Environmental Services, Edinburgh, SA 5111, Australia

* Correspondence: Michael.Short@unisa.edu.au

Received: 11 May 2017; Accepted: 15 June 2017; Published: 19 June 2017

Abstract: The effective control and treatment of acid mine drainage (AMD) from sulfide-containing mine wastes is of fundamental importance for current and future long-term sustainable and cost-effective mining industry operations, and for sustainable management of legacy AMD sites. Historically, AMD management has focused on the use of expensive neutralising chemicals to treat toxic leachates. Accordingly, there is a need to develop more cost-effective and efficient methods to prevent AMD at source. Laboratory kinetic leach column experiments, designed to mimic a sulfide-containing waste rock dump, were conducted to assess the potential of organic waste carbon supplements to stimulate heterotrophic microbial growth, and suppress pyrite oxidation and AMD production. Microbiological results showed that the addition of biosolids was effective at maintaining high microbial heterotroph populations and preventing AMD generation over a period of 80 weeks, as verified by leachate chemistry and electron microscopy analyses. This research contributes to the ongoing development of a cost effective, multi-barrier geochemical-microbial control strategy for reduced mineral sulfide oxidation rates at source.

Keywords: acid mine drainage (AMD); bioremediation; biosolids; heterotrophs; kinetic leach column; organic carbon

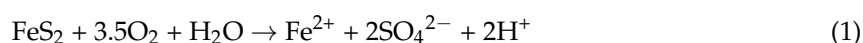
1. Introduction

Mining activities produce large volumes of waste, comprising mainly sub-economic waste rock and tailings. Acid mine drainage (AMD) is generally caused by the accelerated oxidation of pyrite (FeS₂) and other sulfide minerals upon the exposure of these wastes to the atmosphere [1–3]. Consequently, drainage from mining activities is often acidic and is also frequently associated with high concentrations of heavy metals and metalloids—so-called metalliferous drainage.

The release of acidic and metalliferous drainage into neighbouring waterways, streams, and rivers can be severely environmentally damaging [4,5]. Heavy metals, in particular, bioaccumulate in living organisms, causing a range of diseases and disorders [2,6]. AMD, therefore, not only pollutes surface and groundwater bodies, but also degrades the quality of surrounding soil and enables the dispersion of heavy metals into the wider environment [7].

AMD is widely recognised as the biggest environmental issue facing closed and abandoned mines and mine site rehabilitation globally. It presents an impending liability to current and future mining operations worldwide, and also poses a challenge to the environmental and social acceptance of mining activities [8]. In Australia, in 1997, it was estimated that the annual cost for AMD management was AU\$120 M for operating mines with AU\$650 M liability for abandoned mine sites [8–10], with present-day costs expected to be substantially greater. The USA is currently estimated to have more than 557,000 abandoned mines with approximately 15,000 to 23,000 km of streams impacted by AMD. The treatment of these AMD sites for protection of the US natural forest system is estimated to cost about US\$4 billion [11–17]. Total cost estimates for remediating AMD-impacted sites in the USA and Canada combined runs into the tens of billions of dollars [11].

Many value metals, occurring mainly within sulfidic ores, tend to be associated with the generally non-value mineral pyrite—the most abundant sulfide mineral on Earth [2]. Pyrite within waste rocks or tailings when exposed to oxygenated water, undergoes the following reaction resulting in the release of acid [18]:



AMD environments are also frequently associated with elevated temperatures due to the highly exothermic metal sulfide oxidation reactions; pyrite's oxidation enthalpy (Equation (1)) is $-1409 \text{ kJ}\cdot\text{mol}^{-1}$ [19–21]. Yet despite the high level of acidity, heat and high concentrations of toxic metals and metalloids in AMD environments, a diverse range of microorganisms inhabit these systems. AMD microbes, ubiquitous to such environments, are able to survive chemoautotrophically by utilising electrons donated from sulfide minerals, phosphate from water-rock interactions and carbon dioxide (CO_2), oxygen (O_2), and nitrogen (N_2) from the surrounding atmosphere [20].

Early research by Silverman and Ehrlich [22] hypothesised that microorganisms found in AMD environments may in fact be substantially responsible for its generation, with this phenomenon now well established [23]. For example, the activity of iron- and sulfur-oxidising microbes can accelerate the oxidation of pyrite and the subsequent acid generation rate by up to six orders of magnitude [24]. While some chemoautotrophic microbes can exacerbate AMD, other groups of microorganisms, such as heterotrophic bacteria, can form protective biofilms on pyrite surfaces reducing the rate of AMD generation by reducing oxidant (O_2 , ferric iron) availability at the mineral surface and O_2 availability generally within the waters contained in the wastes [23,25]. Accordingly, microbe–mineral interactions are of considerable potential importance for effective and sustainable AMD management; however, such interactions are yet to be fully understood and exploited for AMD control.

The role of silicate in facilitating the formation of stable pyrite surface layers as a geochemical AMD mitigation approach has been studied [26,27]. Research within our own group has demonstrated the effectiveness of geochemical passivation approaches for AMD control: the rate of pyrite oxidation and acid generation were able to be reduced by >97% in synthetic AMD wastes through the formation of silicate stabilised oxy-hydroxide pyrite surface passivation layers at neutral pH [28]. However, such passivation layers can be susceptible to degradation and failure in the long term on pH decrease to below approximately 6 [29]. This suggests that other complementary approaches are needed for effective long-term AMD prevention and control. While the biogeochemical role of microorganisms in AMD production is relatively well studied and understood, the effect of increased abundance of other microbial populations such as heterotrophs, their roles, and metabolic contributions to AMD prevention, is yet to be fully explored [30].

Most AMD environments are classified as oligotrophic (nutrient poor) due to their low concentrations ($<20 \text{ mg}\cdot\text{L}^{-1}$) of dissolved organic carbon [31]. Supplementing these environments with an exogenous organic carbon supply is a common form of biostimulation used to support the growth and activities of beneficial microbial communities such as sulfate-reducers for metals removal in AMD environments [32]. Several studies have recently demonstrated the potential effectiveness of organic carbon supply for heterotrophic stimulation/enrichment for AMD mitigation. For example, the use of various types of manure has been widely explored and found to be effective in promoting the growths

of heterotrophs, and autotrophic anaerobes such as sulfate-reducing bacteria [2,33–38]. Techniques like the co-treatment of municipal wastewater (with biosolids as byproducts) and AMD has recently gained popularity following its introduction by Roetman [39], when it was proposed to remove pathogens in sewage [40]. Results from studies to date have shown the removal of metals, certain nutrients, increases in pH and alkalinity, and overall water/leachates quality improvements [41–50].

In this study we applied a novel at-source AMD control approach in which we mimicked a typical fresh waste rocks dump environment, whilst stimulating heterotrophic microbial growth. We sought to investigate the use of a combined approach coupling microbial stimulation assistance (through the use of biosolids obtained from wastewater treatment), with geochemical pyrite passivation for long-term and sustainable AMD control. Kinetic leach column experiments were run over 84 weeks using a synthetic potentially acid-forming AMD waste, with and without geochemical and microbial interventions to assess the relative efficacy of these approaches. The relative impacts on AMD generation of these treatments are reported in terms of establishment and maintenance of heterotrophic populations, pyrite oxidation (sulfate release), pH and acidity generation.

2. Materials and Methods

2.1. Kinetic Leach Columns

The experimental design consisted of three free-draining kinetic leach columns (KLCs): the Milli-Q water treated control column (Control); a calcite-saturated water column (CSW); and a biosolids-treated column (BS + CSW) (Table 1). Each KLC was set up in duplicate and contained 2 kg of natural minerals (sourced from GeoDiscoveries, West Gosford, NSW, Australia) designed to mimic a typical potentially acid-forming AMD waste, comprising quartz (81.3 wt %), feldspar (10.0 wt %), chlorite (5.0 wt %) and pyrite (3.7 wt %; 2.0 wt % sulfide sulfur) (Table 1). Minerals were crushed to particle sizes of <4 mm. Bulk assay and XRD analyses were performed on individual minerals to confirm their phase purity. Detailed bulk assay results can be found in the Supplementary Materials, Table S1.

The KLC watering/flushing protocol is designed to mimic natural wetting-drying cycles, as detailed in [51]. KLCs were watered (200 mL) every week for three weeks and flushed every fourth week (800 mL) in a continuous cycle. Leachates were collected overnight following flushing events. Heat lamps installed above the columns were operated for 4 h per day on days 4–7 of the weekly cycle to maintain surface temperatures of 30–35 °C and to partially dry the KLC contents between wetting and flushing events.

Phosphate (Na_2HPO_4), to give $0.025 \text{ mg} \cdot \text{P} \cdot \text{L}^{-1}$, was added to the weekly KLC watering/flushing solutions throughout the life of the experiment for both the Control and BS + CSW KLCs to safeguard against potential P-limitation for microbial growth. For the CSW KLC an initial flush at week 0 was carried out using Milli-Q water and thereafter all watering and flushing was carried out using calcite-saturated water (alkalinity $\approx 30 \text{ mg CaCO}_3 \text{ L}^{-1}$). This initial week 0 flush was to prime the KLCs, with subsequent flushes (flush 1 at week 4 and thereafter) collected and analysed. Details on watering and flushing of the BS + CSW KLC are described in Section 2.2. Leachates obtained from the four-weekly flushing cycles were analysed as described in Section 2.4. Solid phase sampling of the Control and BS+CLW KLCs was carried out fortnightly during weeks 0–48 and then every four weeks thereafter to obtain samples for microbiological investigations. Leached pyrite mineral particles were collected from the Control and BS+CLW KLCs at week 84 for surface analysis and imaging.

2.2. Biosolids Leach Column Inoculation and Treatment Solutions

The BS + CSW KLC (biosolids, in conjunction with calcite-saturated water) was designed to investigate the effects of nutrient addition on microbial populations, correlated to leachate chemistry in comparison to the Control and CSW KLCs. The first flush for the BS + CSW KLC at week 0 was carried out using biosolids-augmented calcite-saturated water, and all subsequent watering and flushing also used this solution. The BS + CSW KLC watering/flushing solution comprised a biosolids nutrient

extract using six-month-old biosolids collected from a local wastewater treatment plant in Adelaide, South Australia. The biosolids extract was prepared by leaching a 1:1 mixture of biosolids and Milli-Q water overnight at 4 °C, followed by 0.45 µm filtration for particulates removal. The resulting extract was then aliquoted and frozen (−20 °C) until use. Prior to each weekly application, biosolids extract was diluted in calcite-saturated water to a final concentration of $\approx 140 \text{ mg} \cdot \text{L}^{-1}$ dissolved organic carbon. Details on the chemical characterisation of the biosolids leachate can be found in the Supplementary Materials, Table S2.

The BS + CSW KLC were inoculated with an extract of tailings from a legacy pyrite mine located in Brukunga; 40 km east of Adelaide, South Australia (35°00'26" S 138°56'37" E). Ten grams of Brukunga tailings were vigorously mixed in equal parts of Milli-Q water and applied onto the KLCs as a one-off microbial inoculant.

2.3. Microbiological Analysis

The one-off inoculum used in the BS + CSW KLC was analysed for heterotrophic microbial counts using a standard heterotrophic plate count (HPC) technique. Microbiological analyses using the HPC method was carried out on Control and BS + CSW KLCs fortnightly, in the first half of the leaching experiments. Sampling frequency was then reduced to 4-weekly in the second half of the experiments. The HPC protocol used was modified from [52] and is briefly described herein. Ten grams of sample from each KLC were resuspended in 90 mL sterile pH 7.0 phosphate buffered saline (PBS) (Sigma Aldrich, Castle Hill, NSW, Australia), followed by vigorous agitation for at least 1 min. Culturable cells were enumerated by 10-fold serial dilution using PBS solution, followed by agar plating on R₂A media (Difco Co., Sparks, MD, USA). Plates were incubated at 30 °C for 7 days, with results presented as the number of colony forming units (CFU) per gram of KLC sample. All HPC culturing was performed in duplicate following standard laboratory microbiological protocols.

2.4. Solid Phase Analysis

Quantitative mineralogical analyses were performed using X-ray diffraction (XRD) analysis on a Bruker D4 Endeavor diffractometer with Co K α radiation (1.7902 Å) at 30 kV and 20 mA (Bruker, Billerica, MA, USA; Version 3.0). Phase identification was carried out using the DiffracPlus EVA software (Bruker, Billerica, MA, USA; Version 3.0) with application of the Crystallography Open Database. Quantitative phase analysis was performed using the Rietveld method [53,54], using the TOPAS software (Bruker, Billerica, MA, USA; Version 4.2). Mineral morphology analyses were carried out using environmental scanning electron microscopy (E-SEM; FEI Quanta 450 FEG, Hillsboro, OR, USA) with energy dispersive X-ray spectroscopy (EDS) for semi-quantitative surface chemical composition; both operated at 20 kV.

2.5. Chemistry Analysis of Column Leachates

Leachate fractions collected during flushing events were weighed immediately after collection, with weights used to normalise inductively coupled plasma mass spectrometry (ICP-MS; PerkinElmer, Waltham, MA, USA) concentration data for total S and Fe. The pH, conductivity, redox potential (E_h , all reported relative to the standard hydrogen electrode, SHE) and acidity/alkalinity measurements were conducted at room temperature within 24 h of collection. Acidity/alkalinity was determined after Kirby and Cravotta [55]. Samples for the ICP-MS were acidified and stored at 4 °C until analysis.

2.6. Data and Statistical Analyses

Relationships between measured parameters (pH, E_h , acidity/alkalinity, S, Fe and HPCs) were investigated using parametric Pearson's correlation (alpha significance ≤ 0.05 at 95% CI) in line with underlying data normality assumptions. Where required, data were log₁₀ transformed to meet normality requirements for parametric analyses. Statistical analyses were carried out using Prism® 7.0 (GraphPad Software Inc., La Jolla, CA, USA).

3. Results and Discussion

3.1. KLC Characteristics

Results from mineralogical and microbial analyses at the beginning of the experiments (week 0) are shown in Table 1. The biosolids extract solution assay results showed the presence of various elements including Ca ($950 \text{ mg}\cdot\text{L}^{-1}$), K ($180 \text{ mg}\cdot\text{L}^{-1}$), Mg ($690 \text{ mg}\cdot\text{L}^{-1}$), Na ($870 \text{ mg}\cdot\text{L}^{-1}$), S ($930 \text{ mg}\cdot\text{L}^{-1}$) and Si ($16 \text{ mg}\cdot\text{L}^{-1}$). The complete assay results are reported in Supplementary Materials Table S2. Of note in the raw biosolids leachates was the high conductivity levels, which resulted from the high levels of dissolved Na observed in BS + CSW KLC leachates. HPC analysis performed at day zero showed the presence of heterotrophic microbes in both the Control and BS + CSW KLCs (Table 1; HPC analysis not conducted for the CSW KLC). The BS + CSW KLC contained around 10-fold greater microbial populations at day zero most likely due to inoculation with Brukunga tailings which were not added to the Control KLC.

Table 1. Kinetic leach column (KLC) standard mineral and microbiological compositions at time zero (in wt % unless stated otherwise). Heterotrophic plate count (HPC); colony forming units (CFU); calcite-saturated water column (CSW); biosolids-treated column (BS + CSW).

Components	Phase Impurities	Quantity in KLC	S	C	Fe	Si	HPC (CFU g^{-1})
Quartz	-	81.3	0.04	0.13	0.16	42.7	-
K-feldspar (microcline)	1 quartz	10.0	0.04	0.15	0.06	31.6	-
Chlorite	5 phlogopite	5.0	0.06	0.17	18.00	13.0	-
Pyrite	-	3.7	51.50	0.16	42.80	0.0	-
Calcite	1 quartz	-	0.31	11.84	0.03	0.0	-
Control KLC	-	-	2.00	-	-	-	1×10^4
BS + CSW KLC	-	-	2.00	-	-	-	1.4×10^5
CSW KLC	-	-	2.00	-	-	-	-

3.2. Leachate Analyses

The leachate pH of the Control KLC dropped swiftly from the first flush at week 4 to around pH 4, and continued to decrease before stabilising at pH 2 after around week 8 (Figure 1a). The pH drop can be linked to pyrite oxidation based on the elevated levels of S and Fe leached from the KLC (Figure 1c). An increase in E_h occurred between weeks 4 and 8 from around 600 to 755–851 mV thereafter. This increase in E_h is known to be associated with increase in ferric iron concentrations, alongside decreasing pH ($\text{O}_2 + 4\text{e}^- + 4\text{H}^+ \rightarrow 2\text{H}_2\text{O}$). Each decrease of one pH unit resulted in an increase in E_h of 58 mV, assuming no increase in the presence of other redox couples. Statistical analysis confirmed a negative relationship (-0.776) with an extremely significant correlation ($p < 0.0001$) between pH and E_h (Table 2). The conductivity was variable, averaging $1908 \mu\text{S}\cdot\text{cm}^{-1}$ over the 84-week period (Figure 1b). Unsurprisingly, the leachates from the Control KLC showed increased acidity levels from the second flush at week 8 onwards (Figure 1d), reflecting the lowered pH during this time.

Table 2 shows the results of Pearson correlation analysis for the Control KLC. Statistical analyses of the Control KLC leachates for E_h , conductivity, acidity, S and Fe, showed significant relationships ($p = <0.0001$, <0.0001 , 0.0294 , 0.0015 and 0.0086 , respectively), as a function of pH. On the other hand, no relationship was observed between pH and microbial counts (HPCs), with the negative correlation between these two variables not statistically significant ($p = 0.0882$; Table 2). When all geochemical and microbiological results for the Control KLC leachates (HPCs, pH, E_h , conductivity, acidity, S and Fe) were analysed for possible changes as a function of time, no significant link was found (Table 2).

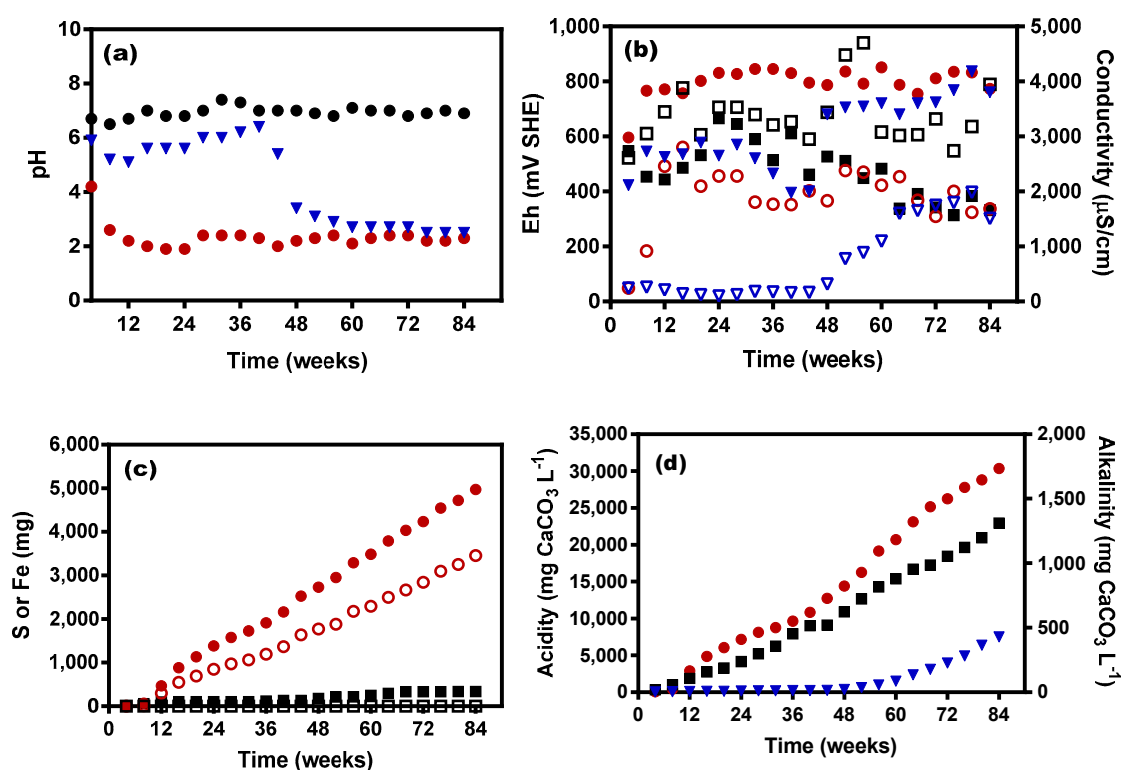


Figure 1. Leachate analyses: (a) Ph; (b) E_h ; (c) cumulative S and Fe in effluents and (d) cumulative acidity and alkalinity. Legend: (a) ●—Control KLC, ▼—CSW KLC, ■—BS + CSW KLC; (b) ●—Control KLC, ▼—CSW KLC; ■—BS + CSW KLC. Secondary y axis (conductivity): ○—Control KLC, ▽—CSW KLC, □—BS + CSW KLC; (c) ●—Control KLC for S, ○—Control KLC for Fe, ■—BS + CSW KLC for S, □—BS + CSW KLC for Fe; (d) ●—Control KLC, ▼—CSW KLC. Secondary y axis (alkalinity): ■—BS + CSW KLC.

Table 2. Pearson correlation coefficients (r) and associated statistical significance level for key parameter correlations in the Control KLC.

Parameter	pH	E_h	Conductivity	Acidity	S	Fe	HPCs
Time	−0.283 ^{ns}	0.385 ^{ns}	0.131 ^{ns}	0.344 ^{ns}	0.167 ^{ns}	0.353 ^{ns}	0.314 ^{ns}
pH		−0.776 ^{***}	−0.788 ^{***}	−0.476 [*]	−0.646 ^{**}	−0.558 ^{**}	−0.391 ^{ns}
S	−0.646 ^{**}	0.250 ^{ns}	0.825 ^{***}	0.840 ^{***}		0.941 ^{***}	−0.013 ^{ns}

Significance level of 2-tailed Pearson r where: ^{ns} not significant, $p \geq 0.05$; ^{*} $p < 0.05$; ^{**} $p < 0.01$; ^{***} $p < 0.001$.

The effluent of the CSW KLC was initially near neutral pH with an average of 5.7 over the first 40 weeks of leaching (Figure 1a). However, the pH dropped sharply after around week 44 while E_h (Figure 1b) and acidity levels (Figure 1d) rose after week 48, demonstrating that calcite-saturated water alone was unable to maintain circumneutral pH and prevent acidity generation in the long term.

The BS + CSW KLC leachates, on the other hand, maintained circumneutral pH over the entire 84 week experimental duration, suggesting effective inhibition of pyrite oxidation as further evidenced by the very low amounts of observed S and Fe dissolution (Figure 1c). Leachate conductivity remained consistently high throughout the life of the experiment (Figure 1c). As detailed earlier, the high conductivity levels in BS + CSW KLC leachates are mostly from dissolved elements like Na present in the original biosolids, rather than being generated from KLC mineral leaching. Further evidence for this assumption comes from statistical analysis (Table 3), which showed no correlation between conductivity and either time, pH or S ($p = 0.6293$, 0.9640 and 0.8515 , respectively). The redox potential (E_h) in the BS + CSW KLC varied in the first 48 weeks of the leaching experiments, averaging

540 mV, dropping afterwards to 393 mV in the final phase of the leaching experiments (beyond week 48) (Figure 1b)—well below the pyrite rest potential (660 mV, SHE). Statistical analysis showed no significant correlations ($p > 0.05$) between pH and any other chemical parameter (Table 3); however, unlike the Control KLC, pH and HPCs were positively correlated ($p = 0.0173$; Table 3).

Table 3. Pearson correlation coefficients (r) and associated statistical significance level for key parameter correlations in the BS + CSW KLC leachate and microbiological results.

Parameter	pH	E_h	Conductivity	Alkalinity	S	Fe	HPCs
Time	0.272 ^{ns}	−0.663 ^{**}	0.112 ^{ns}	0.528 [*]	−0.030 ^{ns}	0	0.571 ^{**}
pH		0.169 ^{ns}	−0.010 ^{ns}	0.268 ^{ns}	−0.208 ^{ns}	0	0.526 [*]
S	−0.208 ^{ns}	−0.218 ^{ns}	−0.044 ^{ns}	0.133 ^{ns}	−	0	−0.072 ^{ns}

Significance level of 2-tailed Pearson r where: ^{ns} not significant, $p \geq 0.05$; ^{*} $p < 0.05$; ^{**} $p < 0.01$.

3.3. Microbial Response to Leachate Changes

There was no significant relationship between pH and heterotrophic microbial populations in the Control KLC ($p = 0.0882$; Table 2). The Control KLC recorded the greatest heterotrophic microbial growth just before week 8, followed by a sudden drop in HPC abundance thereafter (Figure 2a). This apparent link to the decline in pH after week 8 (from pH 4.2 to 2.6) suggests that the microbial community grew initially but could not successfully maintain a stable and abundant population with the onset of adverse physico-chemical conditions (low pH), and most likely insufficient nutrients for microbial growth in the Milli-Q water medium.

Unlike the Control KLC, there was significant positive relationship between pH and HPCs in the BS + CSW KLC ($p = 0.0173$, Table 3), most likely due to the stable neutral pH and consistently high microbial density. Unlike the Control KLC, there was also a positive relationship in microbial growth and survival within the BS + CSW KLC (Figure 2b) as a function of time ($p = 0.0085$, Table 3). The enhanced microbial population as observed in the BS + CSW KLC can be linked to the consistently near-neutral pH levels throughout the life of the experiment, in addition to the consistent nutrient supply (from biosolids) to support heterotrophic microbial growth. No significant link was observed between S and HPCs in either KLC leachate ($p = 0.9567$ and 0.7620 , respectively), suggesting that S levels was not a key parameter affecting heterotrophic microbial populations in these systems. Overall, these results suggest that for biologically-mediated AMD mitigation at source to be effective, a suitable energy (organic carbon) source is needed to stimulate and support heterotrophic microbial populations.

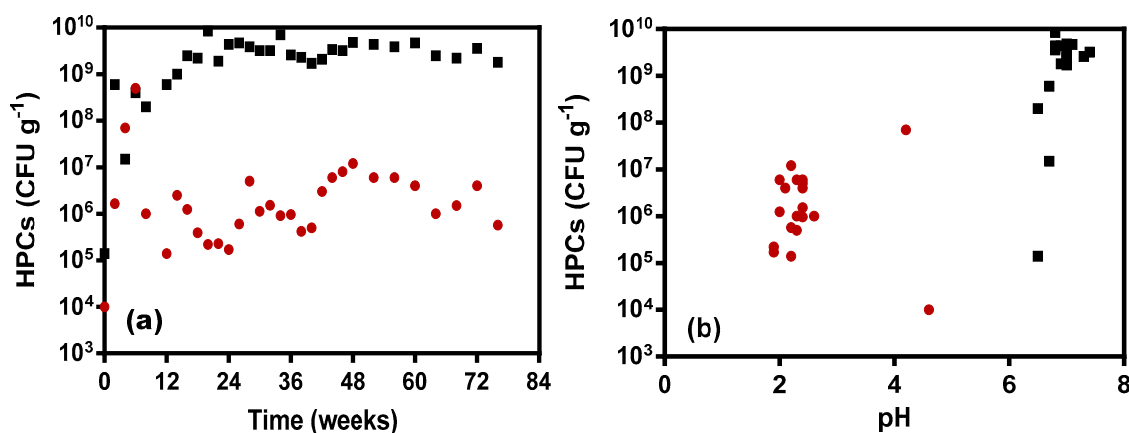


Figure 2. Heterotrophic bacterial counts (log scale; CFU g⁻¹) for Control and BS + CSW KLCs showing (a) microbial population over time and (b) microbial densities as a function of pH (Legend: ●—Control KLC; ■—BS + CSW KLC).

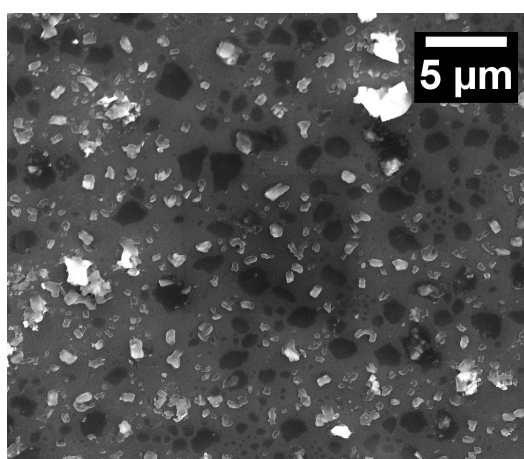
3.4. Microbial O₂ Demand and Reduced Acidity Levels

Regarding the mechanisms of effective microbially mediated pyrite passivation and AMD control in the BS + CSW KLC, it is likely that respiration played an important role, for example via O₂ depletion and/or alkalinity (CO₂) generation. Microbial respiration rates are dependent on the metabolic state (physiological growth phase), and also vary with taxonomic classification. The application of a microbial O₂ uptake rate can provide an indication of likely O₂ consumption patterns in the KLCs. According to figures modified from Wagner et al. [56], the O₂ consumption rate of a typical bacteria (*Escherichia coli*) is 3.6×10^{-13} g O₂ cell⁻¹·day⁻¹. Applying this generic bacterial respiration rate to the average HPC data of the Control and BS + CSW KLCs, the daily O₂ consumption rates of these KLCs are estimated to be 7.4 and 1.01×10^3 mg kg⁻¹·d⁻¹, respectively. This suggests that the microbial respiration rate within the BS + CSW KLC was 1000-fold greater than that within the Control KLC and for the BS + CSW KLC with an internal daily microbial O₂ demand of around 1 g, the in situ O₂ availability for pyrite oxidation could be sufficiently limited.

Correlation analyses showed a significant positive relationship ($r = 0.4954$; $p = 0.0264$) between HPCs and alkalinity in our BS + CSW KLC. While this strong association does not necessarily imply causation from the perspective of heterotrophs increasing the bulk alkalinity through respiration, it does suggest that the two parameters coincide to some extent and that elevated alkalinity (reduced acidity) provides conditions more favourable for the proliferation of heterotrophic microbial populations within this column.

3.5. Pyrite Surface Analyses

E-SEM imaging of pyrite sampled from the Control and BS + CSW KLCs at 84 weeks shows distinctly different surface morphologies (Figure 3). Pyrite from the Control KLC (pH 2.3) showed evidence of oxidation and weathering, with obvious pitting and cracks. Pyrite taken from the BS + CSW KLC (pH 6.9), however, showed no such oxidation or weathering. While no bacteria or biofilms were observed on pyrite surfaces from either KLC, only pyrite from the BS + CSW KLC had a smooth and continuous structure. SEM-EDS analysis confirmed the presence of S, Fe, Si and O on the surfaces of the leached pyrite particles from both KLCs (Figure 3), at week 84. This further suggests that whereas silicate was found to be present in both KLCs, it was only able to form a protective barrier across pyrite from the BS + CSW KLC (Figure 3c).



(a)

Figure 3. Cont.

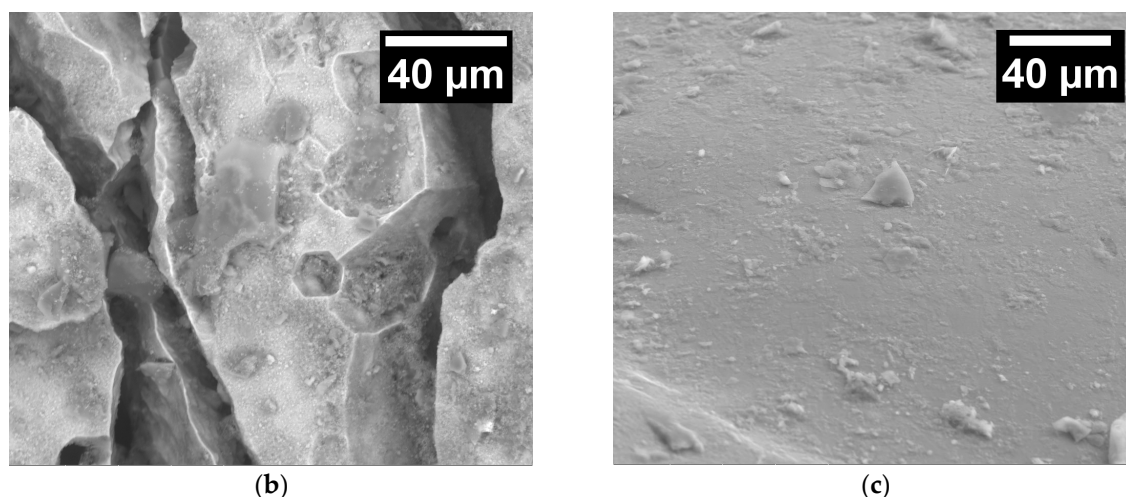


Figure 3. Scanning electron microscope (SEM) micrographs of (a) pyrite at week 0 (45 wt % Fe and 55 wt % S); (b) pyrite from the Control KLC at week 84 (17 wt % O, 44 wt % Fe, 6 wt % Si and 34 wt % S) and (c) pyrite from the BS + CSW KLC at week 84 (20 wt % O, 19 wt % Fe, 8 wt % Si and 53 wt % S).

4. Conclusions

Using a novel approach whereby the growth of heterotrophic microbes was stimulated by the addition of a complex nutrient supply (biosolids) in the presence of low-level alkalinity (calcite-saturated water), AMD was effectively prevented in potentially acid-forming waste rock systems (2 wt % sulfide sulfur) over 84 weeks. In contrast, KLCs supplied with Milli-Q water only failed to maintain neutral pH beyond week 0. Importantly, without the addition of complementary biosolids, low-level alkalinity supply from calcite-saturated water alone (CSW KLC) was not able to prevent acid generation beyond week 44.

Statistical analysis showed a negative relationship and no significant correlation between pH and HPCs in the Control KLCs ($p = 0.0882$). On the other hand, a positive relationship with a significant correlation was observed for the BS + CSW KLC ($p = 0.0173$), with the levels of heterotrophic microbes in the BS + CSW KLC on average some 1000-fold greater than in the Control KLC throughout the experiment. Furthermore, HPCs in the Control KLC showed no significant correlation with time ($p = 0.1783$), but a significant relationship ($p = 0.0085$) was observed for this comparison in the BS + CSW KLC. For the BS + CSW KLC, the continuous supply of a biosolids energy source and low-level alkalinity helped maintain the pH above 6 over the 84-week period, providing a microenvironment that enabled and sustained the growth of heterotrophic microorganisms.

The presence of and increased heterotrophic microbial population appear to be controlling O_2 availability at pyrite surface, hence limiting normal pyrite oxidation and weathering processes. While it was observed that a nutrient supply was effective in boosting heterotrophic microbial populations and passivating pyrite, the exact mechanisms by which this is achieved remain unclear; though it is suggested that O_2 limitation through increased microbial metabolic activities may play a key role in AMD control via pyrite oxidation prevention. Accordingly, heterotrophic microbial stimulation combined with low-level alkalinity supply offers potential to provide effective at-source AMD control.

Whilst our research was focused on the use of biosolids for organic carbon supply, high concentrations of other nutrients like nitrogen associated with a biosolids-based nutrient enrichment may pose other non-AMD environmental challenges (e.g., eutrophication) which would need to be considered prior to any field application. Our work was performed with biosolids addition at $\approx 140 \text{ mg} \cdot \text{L}^{-1}$ dissolved organic carbon, so future work could seek to determine the lower limit of effectiveness for biosolids application in order to minimise any potential ancillary impacts linked to non-carbonaceous nutrients. Future research could also be done to characterise the microbial communities in these systems in order to identify the dominant and active groups, understand the

mechanisms of AMD control (O_2 consumption rates, biofilm formation), and identify the optimal physico-chemical conditions for successful microbially assisted AMD mitigation.

Supplementary Materials: The following are available online at www.mdpi.com/2075-163X/7/6/105/s1, Table S1: Bulk assay results (wt %) of KLC minerals and calcite; Table S2: Biosolids leachates assay results ($mg \cdot L^{-1}$).

Acknowledgments: This research was funded by the Australian Research Council (ARC) linkage project (LP130100568) and co-sponsored by Teck resources (Canada). This research was also supported by an Australian Government Research Training Program (RTP) Scholarship. We also thank AMIRA International (Australia) for their support.

Author Contributions: Omy T. Ogbughalu performed majority of the experimental work, data interpretation and drafted the manuscript. Gujie Qian performed the work for the CSW KLC. Rong Fan and Nobuyuki Kawashima performed the bulk assay on minerals used in the experiment. Omy T. Ogbughalu, Andrea R. Gerson, Roger St. C. Smart, Jun Li and Michael D. Short conceived and designed the research. Andrea R. Gerson, Russell C. Schumann, Jun Li and Michael D. Short edited the manuscript. All authors contributed substantially to research discussions, data interpretation and manuscript drafting.

Conflicts of Interest: The authors declare no conflict of interest.

References

1. Singer, P.C.; Stumm, W. Acidic Mine Drainage: The Rate-Determining Step. *Science* **1970**, *167*, 1121–1123. [[CrossRef](#)] [[PubMed](#)]
2. Johnson, D.B.; Hallberg, K.B. Acid mine drainage remediation options: A review. *Sci. Total Environ.* **2005**, *338*, 3–14. [[CrossRef](#)] [[PubMed](#)]
3. Neculita, C.M.; Zagury, G.J. Biological treatment of highly contaminated acid mine drainage in batch reactors: Long-term treatment and reactive mixture characterization. *J. Hazard. Mater.* **2008**, *157*, 358–366. [[CrossRef](#)] [[PubMed](#)]
4. Murphy, R.; Strongin, D. Surface reactivity of pyrite and related sulfides. *Surf. Sci. Rep.* **2009**, *64*, 1–45. [[CrossRef](#)]
5. Chandra, A.P.; Gerson, A.R. The mechanisms of pyrite oxidation and leaching: A fundamental perspective. *Surf. Sci. Rep.* **2010**, *65*, 293–315. [[CrossRef](#)]
6. Moreno, N.; Querol, X.; Ayora, C.; Pereira, C.F.; Janssen-Jurkovicova, M. Utilization of zeolites synthesized from coal fly ash for the purification of acid mine waters. *Environ. Sci. Technol.* **2001**, *35*, 3526–3534. [[CrossRef](#)] [[PubMed](#)]
7. Hallberg, K.B. New perspectives in acid mine drainage microbiology. *Hydrometallurgy* **2010**, *104*, 448–453. [[CrossRef](#)]
8. Smart, R.S.C.; Miller, S.D.; Stewart, W.S.; Rusdinar, Y.; Schumann, R.E.; Kawashima, N.; Li, J. In situ calcite formation in limestone-saturated water leaching of acid rock waste. *Sci. Total Environ.* **2010**, *408*, 3392–3402. [[CrossRef](#)] [[PubMed](#)]
9. Harries, J. *Acid Mine Drainage in Australia: Its Extent and Potential Future Liability*; Supervising Scientist Report; Office of the Supervising Scientist, Australian Government: Canberra, Australia, 1997; Volume 125, pp. 1–147.
10. Chatwin, T.D. Business case: Gaining a social license to mine—ARD prevention. In *Proceedings of the Sixth Australian Workshop on Acid Drainage*; Bell, L.C., Barrie, B.M.D., Braddock, B., McLean, R.W., Eds.; ACMER, Sustainable Minerals Institute: Brisbane, Australia, 2008; pp. 1–11, ISBN 978-0-9750304-6-2.
11. RoyChowdhury, A.; Sarkar, D.; Datta, R. Remediation of acid mine drainage-impacted water. *Curr. Pollut. Rep.* **2015**, *1*, 131–141. [[CrossRef](#)]
12. United States. *Acid Drainage from Mines on the National Forests: A Management Challenge*; Program aid 1505; Forest Service: Washington, DC, USA; p. 12.
13. USEPA. *Technical Document: Acid Mine Drainage Prediction*; EPA 530-R-94-036, NTIS PB94-201829; Office of Solid Waste: Washington, DC, USA, 1994.
14. Jennings, S.R.; Blicher, P.S.; Neuman, D.R. *Acid Mine Drainage and Effects on Fish Health and Ecology: A Review*; Reclamation Research Group: Bozeman, MT, USA, 2008.
15. USDA Forest Service. Wildland Waters. Issue 4. Winter 2005; FS-812. Available online: <http://www.fs.fed.us> (accessed on 1 May 2017).

16. Kim, A.; Heisey, B.; Kleinmann, R.; Deul, M. *Acid Mine Drainage: Control and Abatement Research. Information circular/1982*; Pittsburgh Research Center: Pittsburgh, PA, USA, 1982.
17. Benner, S.G.; Blowes, D.W.; Ptacek, C.J. A Full-Scale Porous Reactive Wall for Prevention of Acid Mine Drainage. *Groundw. Monit. Remediat.* **1997**, *17*, 99–107. [[CrossRef](#)]
18. Adams, D.J.; Ogden, U.T.; Pennington, P.; Tachie-Menson, S.; Gutierrez, L.A.F. The role of microorganisms in acid rock drainage. In Proceedings of the SME Annual Meeting, Salt Lake City, UT, USA, 28 February–2 March 2005.
19. Rohwerder, T.; Schippers, A.; Sand, W. Determination of reaction energy values for biological pyrite oxidation by calorimetry. *Thermochim. Acta* **1998**, *309*, 79–85. [[CrossRef](#)]
20. Baker, B.J.; Banfield, J.F. Microbial communities in acid mine drainage. *FEMS Microbiol. Ecol.* **2003**, *44*, 139–152. [[CrossRef](#)]
21. Lefebvre, R.; Hockley, D.; Smolensky, J.; Gélinas, P. Multiphase transfer processes in waste rock piles producing acid mine drainage: 1: Conceptual model and system characterization. *J. Contam. Hydrol.* **2001**, *52*, 137–164. [[CrossRef](#)]
22. Silverman, M.P.; Ehrlich, H.L. Microbial Formation and Degradation of Minerals. In *Advances in Applied Microbiology*; Wayne, W.U., Ed.; Academic Press: Cambridge, MA, USA, 1964; pp. 153–206.
23. Johnson, D. Recent Developments in Microbiological Approaches for Securing Mine Wastes and for Recovering Metals from Mine Waters. *Minerals* **2014**, *4*, 279–292. [[CrossRef](#)]
24. Evangelou, V.P.; Zhang, Y.L. A review: Pyrite oxidation mechanisms and acid mine drainage prevention. *Crit. Rev. Environ. Sci. Technol.* **1995**, *25*, 141–199. [[CrossRef](#)]
25. Afzal Ghauri, M.; Okibe, N.; Johnson, D.B. Attachment of acidophilic bacteria to solid surfaces: The significance of species and strain variations. *Hydrometallurgy* **2007**, *85*, 72–80. [[CrossRef](#)]
26. Schumann, R. Passivating surface layer formation on pyrite in neutral rock drainage. In Proceedings of the 8th International Conference on Acid Rock Drainage (ICARD) and Securing the Future: Mining, Metals & the Environment in a Sustainable Society 2009, Skelleftea, Sweden, 22–26 June 2009.
27. Miller, S.D.; Schumann, R.; Smart, R.; Rusdinar, Y. ARD Control by Limestone Induced Armouring and Passivation of Pyrite Minerals Surfaces. In Proceedings of the 8th International Conference on Acid Rock Drainage (ICARD) and Securing the Future: Mining, Metals & the Environment in a Sustainable Society 2009, Skelleftea, Sweden, 22–26 June 2009.
28. Fan, R.; Schumann, R.; Smart, R.; Rusdinar, Y. The formation of surface passivating layers on pyrite for reduced acid rock drainage. *Environ. Sci. Technol* **2017**, submitted.
29. Zeng, S.; Li, J.; Schumann, R.; Smart, R. Effect of pH and dissolved silicate on the formation of surface passivation layers for reducing pyrite oxidation. *Comput. Water Energy Environ. Eng.* **2013**, *2*, 50. [[CrossRef](#)]
30. Gerson, A.R.; Li, J.; Smart, R.S.C.; Saint, C.P.; Short, M.D.; Schumann, R.C.; Jarvie-Eggart, M.; Muga, H. *Responsible Management of Acid Mine Wastes: Geochemical and Microbiological Resources*; SME Publications: Littleton, CO, USA, 2014; pp. 519–524.
31. Johnson, D.B. Biodiversity and ecology of acidophilic microorganisms. *FEMS Microbiol. Ecol.* **1998**, *27*, 307–317. [[CrossRef](#)]
32. Lefevre, E.; Pereyra, L.P.; Hiibel, S.R.; Perrault, E.M.; De Long, S.K.; Reardon, K.F.; Pruden, A. Molecular assessment of the sensitivity of sulfate-reducing microbial communities remediating mine drainage to aerobic stress. *Water Res.* **2013**, *47*, 5316–5325. [[CrossRef](#)] [[PubMed](#)]
33. Behum, P.T.; Lefticariu, L.; Bender, K.S.; Segid, Y.T.; Burns, A.S.; Pugh, C.W. Remediation of coal-mine drainage by a sulfate-reducing bioreactor: A case study from the Illinois coal basin, USA. *Appl. Geochem.* **2011**, *26*, S162–S166. [[CrossRef](#)]
34. Lindsay, M.B.; Blowes, D.W.; Condon, P.D.; Ptacek, C.J. Organic carbon amendments for passive in situ treatment of mine drainage: Field experiments. *Appl. Geochem.* **2011**, *26*, 1169–1183. [[CrossRef](#)]
35. McMahon, M.J.L.; Daugulis, A.J. Enhancement of biogenic sulfide production in a packed-bed bioreactor via critical inoculum design and carrier material selection. *Biotechnol. Bioeng.* **2008**, *100*, 855–863. [[CrossRef](#)] [[PubMed](#)]
36. Neculita, C.-M.; Zagury, G.J.; Bussière, B. Passive treatment of acid mine drainage in bioreactors using sulfate-reducing bacteria. *J. Environ. Qual.* **2007**, *36*, 1–16. [[CrossRef](#)] [[PubMed](#)]
37. Postgate, J.R. *The Sulphate Reducing Bacteria*, 2nd ed.; Cambridge University Press: Cambridge, UK, 1984.

38. Widdel, F. Microbiology and Ecology of Sulfate- and Sulfur-Reducing Bacteria. In *Biology of Anaerobic Microorganisms*; John Wiley & Sons: New York, NY, USA, 1988; pp. 469–585.
39. Roetman, E.T. The sterilization of sewage by acid mine water. Master's Thesis, West Virginia University, Morgantown, WV, USA, 1932.
40. Deng, D.; Weidhaas, J.L.; Lin, L.-S. Kinetics and microbial ecology of batch sulfidogenic bioreactors for co-treatment of municipal wastewater and acid mine drainage. *J. Hazard. Mater.* **2016**, *305*, 200–208. [[CrossRef](#)] [[PubMed](#)]
41. Johnson, K.L.; Younger, P.L. The co-treatment of sewage and mine waters in aerobic wetlands. *Eng. Geol.* **2006**, *85*, 53–61. [[CrossRef](#)]
42. McCullough, C.D.; Lund, M.A.; May, J.M. Field-scale demonstration of the potential for sewage to remediate acidic mine waters. *Mine Water Environ.* **2008**, *27*, 31–39. [[CrossRef](#)]
43. Wei, X.; Viadero, R.C.; Bhojappa, S. Phosphorus removal by acid mine drainage sludge from secondary effluents of municipal wastewater treatment plants. *Water Res.* **2008**, *42*, 3275–3284. [[CrossRef](#)] [[PubMed](#)]
44. Strosnider, W.H.; Winfrey, B.K.; Nairn, R.W. Novel passive co-treatment of acid mine drainage and municipal wastewater. *J. Environ. Qual.* **2011**, *40*, 206–213. [[CrossRef](#)] [[PubMed](#)]
45. Strosnider, W.; Winfrey, B.; Nairn, R. Alkalinity generation in a novel multi-stage high-strength acid mine drainage and municipal wastewater passive co-treatment system. *Mine Water Environ.* **2011**, *30*, 47–53. [[CrossRef](#)]
46. Strosnider, W.; Winfrey, B.; Nairn, R. Biochemical oxygen demand and nutrient processing in a novel multi-stage raw municipal wastewater and acid mine drainage passive co-treatment system. *Water Res.* **2011**, *45*, 1079–1086. [[CrossRef](#)] [[PubMed](#)]
47. Ruihua, L.; Lin, Z.; Tao, T.; Bo, L. Phosphorus removal performance of acid mine drainage from wastewater. *J. Hazard. Mater.* **2011**, *190*, 669–676. [[CrossRef](#)] [[PubMed](#)]
48. Winfrey, B.; Strosnider, W.; Nairn, R.; Strevett, K. Highly effective reduction of fecal indicator bacteria counts in an ecologically engineered municipal wastewater and acid mine drainage passive co-treatment system. *Ecol. Eng.* **2010**, *36*, 1620–1626. [[CrossRef](#)]
49. Strosnider, W.; Winfrey, B.; Peer, R.; Nairn, R. Passive co-treatment of acid mine drainage and sewage: Anaerobic incubation reveals a regeneration technique and further treatment possibilities. *Ecol. Eng.* **2013**, *61*, 268–273. [[CrossRef](#)]
50. Younger, P.L.; Henderson, R. Synergistic wetland treatment of sewage and mine water: Pollutant removal performance of the first full-scale system. *Water Res.* **2014**, *55*, 74–82. [[CrossRef](#)] [[PubMed](#)]
51. Smart, R.; Skinner, B.; Levay, G.; Gerson, A.; Thomas, J.; Sobieraj, H.; Schumann, R.; Weisener, C.; Weber, P.; Miller, S. *ARD Test Handbook*; AMIRA International: Melbourne, Australia, 2002.
52. Pepper, I.L.; Zerkhi, H.G.; Bengson, S.A.; Iker, B.C.; Banerjee, M.J.; Brooks, J.P. Bacterial populations within copper mine tailings: Long-term effects of amendment with Class A biosolids. *J. Appl. Microbiol.* **2012**, *113*, 569–577. [[CrossRef](#)] [[PubMed](#)]
53. Rietveld, H. Line profiles of neutron powder-diffraction peaks for structure refinement. *Acta Crystallogr.* **1967**, *22*, 151–152. [[CrossRef](#)]
54. Rietveld, H. A profile refinement method for nuclear and magnetic structures. *J. Appl. Crystallogr.* **1969**, *2*, 65–71. [[CrossRef](#)]
55. Kirby, C.S.; Cravotta, C.A. Net alkalinity and net acidity 2: Practical considerations. *Appl. Geochem.* **2005**, *20*, 1941–1964. [[CrossRef](#)]
56. Wagner, B.A.; Venkataraman, S.; Buettner, G.R. The rate of oxygen utilization by cells. *Free Radic. Biol. Med.* **2011**, *51*, 700–712. [[CrossRef](#)] [[PubMed](#)]

